Status of the general description of fission observables by the GEF code

B. Jurado[1] and K.-H. Schmidt[1]
[1]CENBG, CNRS/IN2P3, Chemin du Solarium, B. P. 120, 33175 Gradignan, France

Abstract
The GEneral Fission (GEF) model treats spontaneous fission and fission up to an excitation energy of about 100 MeV of a wide range of heavy nuclei. GEF makes use of general laws of statistical and quantum mechanics, assuring a high predictive power. It is unique in providing a general description of essentially all fission observables in a consistent way while preserving the correlations between all of them. In this contribution we present some of the physical aspects on which the model is based, give an overview on the results that can be obtained with the code and show an example that illustrates how the GEF code can serve as a framework for revealing the sensitivity of the fission observables to some basic nuclear properties.

1 Introduction

During several short-term visits that were financed by the EFNUDAT and by the ERINDA projects, the semi-empirical GEneral Fission model GEF has been developed and continuously extended. The GEF code provides results for fissioning nuclei ranging from polonium to seaborgium up to excitation energies of 100 MeV including multi-chance fission. Contrary to most of the existing fission models, GEF gives also reliable results for nuclei where no experimental information is available. GEF is a Monte-Carlo code and calculates for each fission event all the properties of the two fission fragments at scission: mass, charge, excitation energy and angular momentum, as well as the fission-fragment kinetic energies. In addition, GEF treats the deexcitation of the fission fragments and provides the prompt-neutron and prompt-gamma multiplicities associated with each fragment, as well as the prompt-neutron and prompt-gamma kinetic energies and angles. All this information can be delivered by the code on an event-by-event basis and can serve as an event generator for simulation purposes. Because the model is based on robust physical concepts, one can also make use of the correlations between the different physical quantities given by GEF.

2 Physics behind GEF

GEF combines general laws of quantum and statistical mechanics with specific experimental information. A complete description of the code can be found in [1]. In this contribution we concentrate on the main ideas used to derive the global shape of the fission-fragment yields and the partition of the intrinsic excitation energy between the fragments.

2.1 Fission-fragment yields

The fission-fragment yields are determined by the potential energy landscape between the fission barrier and scission as a function of the mass-asymmetry degree of freedom. The microscopic-macroscopic approach has proven to be very useful for calculating nuclear properties, in particular in applications to fission [2]. According to this approach, the shape of the potential

energy on the way to scission is given by the combination of the macroscopic potential, as given by the liquid-drop model, and shell effects. When the two-centre shell model became available, it was possible to study the single-particle structure in a di-nuclear potential with a necked-in shape. Investigations of Mosel and Schmitt [3] revealed that the single-particle structure in the vicinity of the outer fission barrier already resembles very much the sequence of single-particle levels in the two separated fragments. They explained this result by the general quantum-mechanical feature that wave functions in a necked-in potential are already essentially localized in the emerging fragments. This finding means that the microscopic properties of the fissionning system are essentially determined by the shells of the fragments, and only the macroscopic properties are specific to the fissioning system [4]. This "separability principle" is exploited in the GEF code, which relies on empirical information to determine the stiffness of the macroscopic potential and the position and strength of the fragment shells. The latter are valid for all fissioning systems, which explains why the GEF code is able to give results for a very large number of fissioning nuclei with just one single set of parameters. The magnitudes of the shell effects that form the fission valleys and the stiffness parameters in mass-asymmetric distortions are deduced from a global fit of measured mass distributions.

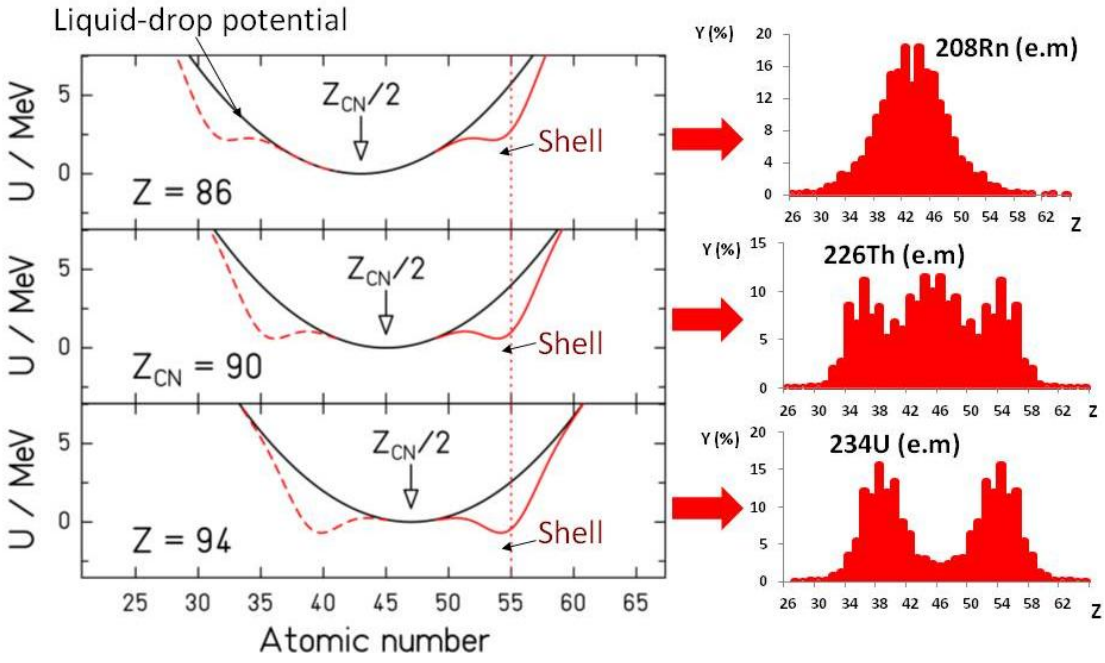

Fig. 1: (Left) Total potential energy (red lines) and macroscopic potential (black lines) as a function of the fragment charge for fissioning nuclei around Th with steps of $4Z_{CN}$ (schematic). The minimum of the macroscopic potential located at symmetry is indicated. One fragment shell located at Z=55 is assumed. (Right) Corresponding variation of the experimental charge distributions around ^{226}Th obtained in electromagnetic-induced fission [5].

Regarding shell effects, asymmetric fission was initially attributed to the influence of a deformed ($\beta\approx0.6$) fragment shell at N=88 and the combined influence of the spherical shells at N=82 and Z=50 [6]. However, new data on fission-fragment Z distributions over long isotopic chains [7], reveal very clearly that the position in neutron number varies systematically over more than 7 units, while the position in proton number is approximately constant at Z=54. The rather short isotopic sequences covered in former experiments did not show this feature clearly enough and gave the false impression of a constant position in mass. This finding represents a severe

puzzle to theory, since shell-model calculations [6, 8] do not show any shell stabilization near Z=54 at a deformation of $\beta \approx 0.6$, which is suggested by the mass-dependent prompt-neutron yields, see below. Therefore, the shell effect close to Z=54 is a key input information included in GEF that has a purely empirical origin. Fig. 1 illustrates how the observed transition from symmetric to asymmetric fission around A=226 can be explained by the interplay between the macroscopic potential and shell effects. The strength of the shell and its position is fixed for the three fissioning nuclei considered. However, the stiffness and the position of the minimum of the macroscopic potential increase with the mass of the fissioning nucleus. As a consequence, the minimum of the total potential moves from symmetric to asymmetric splits.

2.2 Partition of excitation energy between the fragments

The early manifestation of fragment shells on the fission path, mentioned above, indicates that the fragments acquire their individual characteristics already in the vicinity of the fission barrier. Therefore, at this position the fissioning nucleus consists of two well defined nuclei in contact through the neck. Before scission, the available intrinsic excitation energy E^*_{intr} (given by the sum of excitation energy above the barrier and the dissipated potential energy after the sadle) has to be divided between the fragments. In GEF the excitation-energy partition is determined according to statistical mechanics. It is assumed that the system formed by the two nuclei in contact reaches statistical equilibrium where all the configurations that are energetically possible have the same probability to be populated. Therefore, the partition of excitation energy is determined by a probability distribution that is given by the product of the level densities of the individual fragments. The average excitation energy of the light fragment $<E_L>$ at thermal equilibrium of the light fragment is given by :

$$< E_L >= \frac{\int_0^{E^*_{intr}} E_L \rho_L(E_L)\rho_H(E^*_{intr} - E_L)dE_L}{\int_0^{E^*_{intr}} \rho_L(E_L)\rho_H(E^*_{intr} - E_L)dE_L}. \qquad (1)$$

where ρ_L and ρ_H are the level densities of the light and heavy fragment, respectively.

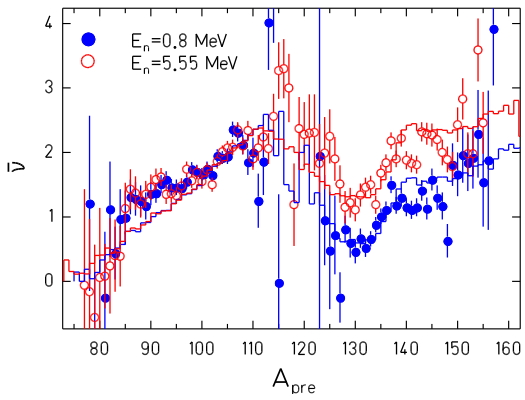

Fig. 2: Measured prompt-neutron yield in ^{237}Np(n,f) as a function of pre-neutron mass at two different incident-neutron energies [9] (data points) in comparison with the result of the GEF code (histograms).

There is increasing evidence [10, 11] that the nuclear level density in the regime of pairing correlations essentially deviates from the widely so-called Fermi-gas level-density formula that had been derived by Bethe [12] for a system of non-interacting Fermions. Due to the gradual

breaking of Cooper pairs, the effective number of degrees of freedom of the nucleus increases strongly, leading to a large heat capacity, and, therefore, the level density as a function of excitation energy is well approximated by an exponential function. This means that the nuclear temperature in the regime of pairing correlations is essentially constant. Thus, the fissioning nucleus represents a very interesting system of two microscopic objects that behave as coupled thermostats with a limited total energy. Because the logarithmic slope of the level densities in the constant-temperature regime is proportional to $A^{2/3}$, the most probable configurations are those where the available excitation energy concentrates in the heavy fragment. In other words, excitation-energy sorting takes place, where the thermal energy is transferred from the light to the heavy fragment [13-15]. The process of energy sorting is clearly reflected by experimental data on prompt-neutron yields. Fig. 2 shows the prompt-neutron yields of the system ^{237}Np(n,f) for two energies of the incoming neutrons. The additional energy introduced by the 5.5-MeV neutrons enhances the prompt-neutron yields in the heavy fission-fragment group, only, while the neutron yields in the light group remain unchanged. Of course, the energy-sorting process ends at scission, and the deformation energy of the individual fragments at scission, that is dissipated after scission, remains in the respective fragment and represents the main source of the saw-tooth like behaviour of the mean mass-dependent prompt-neutron fission yield. In [16] we show that the even-odd effect in fission-fragment elemental yields is the consequence of extreme excitation-energy sorting, i.e., the even-odd effect reflects the preferential population of the ground state of even-even light fragments.

3 Comparison with experimental data and evaluations

In the following figures the results obtained with GEF are compared with experimental data. All the GEF results have been obtained with the same parameter set. Fig. 3 shows the fission-fragment distributions for different systems ranging from the electromagnetic-induced fission of ^{226}Th to the spontaneous fission of ^{258}Fm. It is remarkable that fine structure effects such as the even-odd staggering of the elemental yields of ^{226}Th and the very fast transition from asymmetric to symmetric fission observed when going from ^{256}Fm to ^{258}Fm are very well reproduced by GEF.

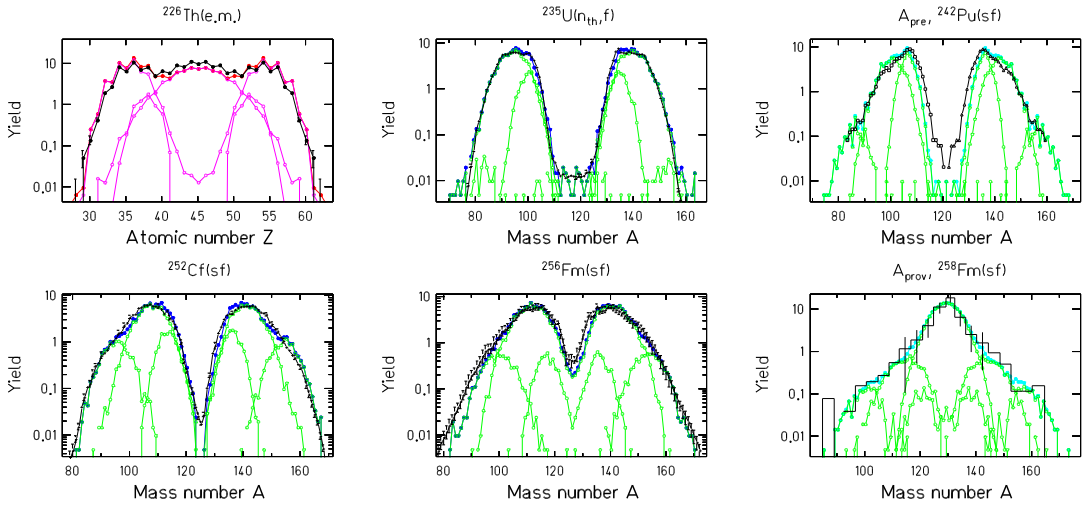

Fig. 3: Mass and Z distributions of fission fragments from spontaneous fission (sf), thermal-neutron-induced fission (n_{th},f) and electromagnetic-induced fission (e.m.). (In most cases the post-neutron masses are shown. A_{prov} is the "provisional mass" that is directly deduced from the ratio of the kinetic energies of the fragments and, thus, it is not corrected for neutron emission.) Measured or evaluated data (black lines, respectively histogram) are compared with predictions of the GEF code (pink and green lines). The contributions of different fission channels are shown. (See [1] for references of the data.)

Fig. 4 shows the variation of the average prompt-neutron multiplicities with incident neutron energy for various fissionning nuclei. The differences between GEF results and the values given by ENDF/B-VII.1 amount to less than 0.2 neutrons for all systems. Note that the prompt-neutron multiplicity is a very complex quantity that strongly depends on the particular shape of the fragment yields and on the properties of the fragments at scission. It is not possible to simply extrapolate this quantity from one fissioning nucleus to another because the shapes of the yields can strongly vary for neighbouring fissioning nuclei, as shown for instance for ^{256}Fm and ^{258}Fm in Fig. 3. GEF results for the average number of neutrons as a function of the fragment mass for ^{237}Np at two incident neutron energies are presented in Fig. 2. The increase of the neutron yields of the heavy fragments when the incident energy increases is very well reproduced by GEF thanks to the inclusion of the energy-sorting process.

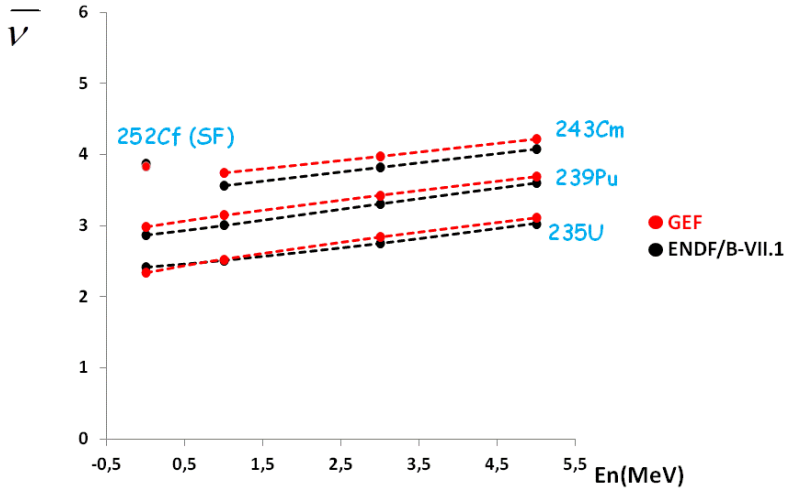

Fig. 4: Average prompt-neutron multiplicities as a function of neutron energy for different fissioning nuclei.

The experimental prompt fission-neutron spectrum for the system ^{235}U(n_{th},f) [17] is compared with results of the GEF code in Fig. 5. In order to better visualize the deviations, the right panel shows a reduced presentation with the spectrum normalized to a Maxwellian distribution with the parameter T= 1.32 MeV. The GEF code reproduces the data very well. Good agreement has also been found with the experimental fission-prompt-neutron spectra of ^{252}Cf(sf), ^{240}Pu(sf) and ^{239}Pu(n_{th},f) [1]. This qualifies the GEF code for estimating prompt-neutron spectra in cases where experimental data do not exist. It also seems to be a suitable tool for improving evaluations.

4 GEF: a useful tool for reactor physics

The previous figures show that GEF has acquired an accuracy that meets the requirements of technical applications. Indeed, GEF fission-fragment yields will be part of the next edition of the JEFF library. Moreover, different features have been developed to facilitate the use of GEF results in reactor physics. The most important ones are:

-The independent and cumulative yields of GEF are available in ENDF format (GEFY) [18].

-There is also a deterministic version of GEF in the form of a subroutine (GEFSUB) that can be linked to deterministic codes like e.g. TALYS or EMPIRE [1].

-Error bars for yields from perturbed model parameters including the covariance matrix for yields are available [1]. The covariance matrix is determined by the correlations between the yields of different nuclides according to the underlying physics of the model.

-GEF also calculates the production of isomers [1].

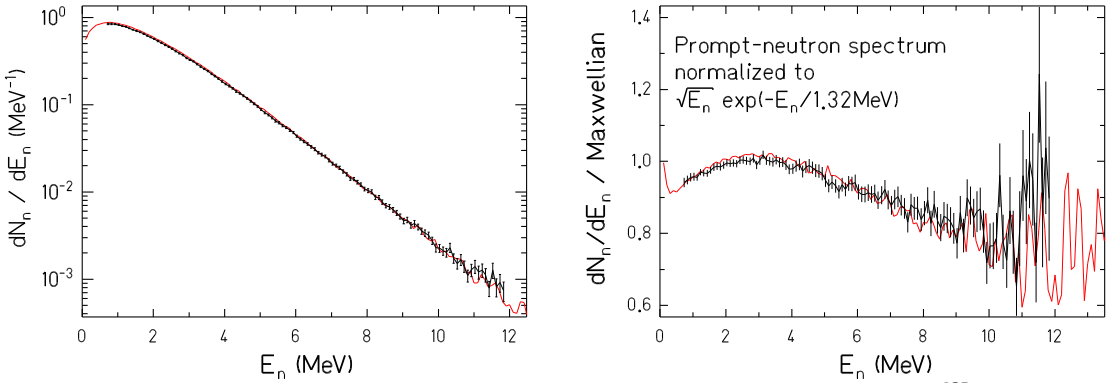

Fig. 5: Experimental prompt-fission-neutron spectra (black lines and error bars) for ^{235}U(n_{th},f) [17] in comparison with the result of the GEF code (red lines). In the right panel the spectra have been normalized to a Maxwellian with T = 1.32 MeV.

5 GEF: a useful tool for fundamental physics

As has been shown above, the GEF model has been developed within a global approach where the same description is used for all fissioning nuclei. There is no local parameter adjustment and the tuning of the model parameters within a certain region of fissioning nuclei has naturally an impact also for fissioning systems located in a different region. This is a powerful feature that can help to reveal some basic nuclear properties. In this contribution we will illustrate how the GEF code has revealed the presence of a shell effect at Z=44. The accurate reproduction by GEF of the mass distribution for ^{239}Pu(n_{th},f) and other neighbouring fissioning nuclei can only be obtained by the inclusion of a shell effect at Z=44 that increases the yields in the light-fragment side close to A~105 and the complementary heavy fragments. This shell has no mayor impact for lighter actinides. However, it has a significant influence on the yields of relatively light neutron-deficient fissioning nuclei like ^{180}Hg, where an asymmetric mass distribution has recently been measured [19]. As can be seen in Fig. 6, the mass distribution given by GEF changes from a symmetric to an asymmetric shape when the shell effect at Z=44 is included. The asymmetric distribution shown on the right part of Fig. 6 has been calculated assuming an excitation energy of 12 MeV. However, in the measurement the ^{180}Hg nuclei are populated after the beta decay of ^{180}Tl. They follow an excitation-energy distribution that is not well defined and can cover energies below and above 12 MeV. This can explain, at least partly, the differences found between GEF and the data on the right panel of Fig. 6.

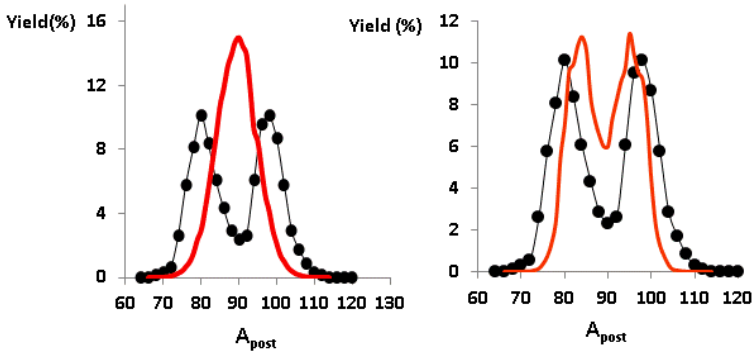

Fig. 6: Experimental post-neutron fission-fragment mass distribution of ^{180}Hg [19] (black dots) compared to GEF results (red lines). The shell effect at Z=44 is only included in the GEF calculation shown in the right panel.

6 Conclusions and perspectives

The GEF model gives reliable predictions for essentially all fission observables of a broad range of fissioning nuclei, including nuclei where no experimental data exist. The GEF model combines physical concepts from quantum mechanics and statistical mechanics with specific experimental information within a general approach where the same description is applied to all the fissioning systems. In this contribution we have shown that GEF results are in good agreement with experimental data on fission-fragment distributions, prompt-neutron yields and prompt-neutron energy spectra of different fissioning nuclei. The accuracy of GEF meets the requirements of technical applications. As a consequence, fission-fragment yields given by GEF will be included in the next edition of the JEFF library. GEF can also be very useful for investigating fundamental nuclear properties. As an example, GEF has revealed the existence of a shell effect at Z=44 that has some influence on the fission-fragment mass distributions of heavy actinides like ^{239}Pu and explains the asymmetric character of the mass distribution of light neutron-deficient nuclei such as ^{180}Hg.

GEF is constantly improved. Some of the foreseen developments are the inclusion of ternary fission, the treatment of proton-, electron- and photon-induced fission and the incorporation of more detailed nuclear-structure information of the fission fragments. We will also perform a quantitative assessment of the deviations between GEF and experimental and evaluated data.

Acknowledgement

This work was supported by the European Commission within the Sixth Framework Programme through EFNUDAT (project no. 036434) and within the Seventh Framework Programme through Fission-2010-ERINDA (project no. 269499), and by the NEA of the OECD.

References

[1] http://www.cenbg.in2p3.fr/GEF or http://www.khs-erzhausen.de/GEF (and references therein)
[2] M. Brack et al., Rev. Mod. Phys. **44**, 320 (1972)
[3] U. Mosel, H. W. Schmitt, Nucl. Phys. A **165,** 73 (1971)
[4] K.-H. Schmidt, A. Kelic, M. V. Ricciardi, Europh. Lett. **83**, 32001 (2008)
[5] K.-H. Schmidt et al., Nucl. Phys. A **665**, 221 (2000)
[6] B. D. Wilkins, E. P. Steinberg, R. R. Chasman, Phys. Rev. C **14,** 1832 (1976)
[7] C. Boeckstiegel et al., Nucl. Phys. A **802**, 12 (2008)
[8] I. Ragnarsson, R. K. Sheline, Phys. Scr. **29**, 385 (1984)
[9] A. A. Naqvi, F. Kaeppeler, F. Dickmann, R. Mueller, Phys. Rev. C **34,** 218 (1986)
[10] M. Guttormsen et al., Phys. Rev. C **68**, 034311 (2003)
[11] K.-H. Schmidt, B. Jurado, Phys. Rev. C **86**, 044322 (2012)
[12] H. A. Bethe, Phys. Rev. **50**, 332 (1936)
[13] K.-H. Schmidt, B. Jurado, Phys. Rev. Lett. **104**, 212501 (2010)
[14] K.-H. Schmidt, B. Jurado, Phys. Rev. C **83**, 014607 (2011)
[15] K.-H. Schmidt, B. Jurado, Phys. Rev. C **83**, 061601 (2011)
[16] K.-H. Schmidt, B. Jurado, submitted to Phys. Rev. Lett.
[17] N. V. Kornilov et al., Nucl. Science Engin. **165**, 117 (2010)

[18] http://www.cenbg.in2p3.fr/GEFY or http://www.khs-erzhausen.de/GEFY
[19] A. N. Andreyev et al., Phys. Rev. Lett. **105**, 252502 (2010)